

CANOPY EVAPOTRANSPIRATION, LEAF TRANSPIRATION AND WATER USE EFFICIENCY OF AN ANDEAN PASTURE IN SE-ECUADOR – A CASE STUDY

BRENNER SILVA, SIMONE STROBL, ERWIN BECK and JÖRG BENDIX

With 7 figures and 3 tables

Received 21 July 2015 · Accepted 05 January 2016

Summary: The relationship between canopy-level evapotranspiration (ET_{Sci}) and leaf-level transpiration (T_{leaf}) as well as photosynthesis (P_{leaf}) for a homogeneous tropical montane pasture was analyzed over five days using a combination of methods involving a laser scintillometer and a porometer. Weather conditions ranged from overcast to sunny during the period of study. The gas exchange of the leaves of the dominant pasture grass *Setaria sphacelata* (transpiration vs. photosynthetic CO_2 net uptake) was measured with a porometer and physiologically interpreted on the background of microclimate variables (photosynthetic active radiation (PAR) as proxy for total light intensity, temperature, water vapor deficit of the air) and soil moisture data. Water use efficiency (WUE, photosynthetic CO_2 net uptake vs water loss by leaf transpiration) of the pasture was used to analyze the grass' range of response to the environmental variables of the research area. PAR and water vapor deficit of the air (VPD) appeared to be the determinant factors for T_{leaf} and ET_{Sci} . WUE for the *Setaria sphacelata* pasture ranged from 1.9 to 5.8 $\mu mol CO_2 mmol^{-1} H_2O day^{-1}$ and is particularly low during periods of high VPD combined with enhanced insolation during cloudless periods. ET measurements collected by the scintillometer demonstrated a strong correlation with water flux calculated using the Penman-Monteith approach (T_{PM}) ($r^2 = 0.95$). Also, T_{leaf} measured with the porometer showed reasonable coincidence with the ET observations ($r^2 = 0.78$). Values of ET_{Sci} ranged from 2.26 to 4.96 $mm day^{-1}$ and T_{leaf} ranged from 0.83 to 2.41 $mm day^{-1}$, but only ET_{Sci} showed good correspondence with the available energy (net radiation). The lower correlation between T_{leaf} and canopy-level ET_{Sci} compared to that between ET_{Sci} and T_{PM} was tested against contaminations from the adjacent fetch area of the scintillometer path, but no effects were found. Likewise, soil water limitations of T_{leaf} could be ruled out. Therefore, different correlations of ET_{Sci} and T_{leaf} with the incoming energy and VPD may be traced back to a direct effect of the VPD on ET in contrast to its indirect effect on T_{leaf} which is additionally regulated by physiological processes in the leaf stomata.

Zusammenfassung: Eine Kombination von Laser-Szintillometer- und Porometer-Messungen wurde verwendet, um die Beziehung zwischen der Pfad-Evapotranspiration (ET_{Sci}) und der Blatt-Transpiration (T_{leaf}) sowie der photosynthetischen Netto- CO_2 Aufnahme (P_{leaf}) für eine homogene tropisch-montane Weidefläche zu analysieren. Die Messungen erfolgten an fünf Tagen mit unterschiedlichen Wetterbedingungen (bewölkt bis wolkenfrei). Der Gasaustausch der Blätter des dominierenden Weidegrases *Setaria sphacelata* (Photosynthese- CO_2 -Nettoaufnahme versus Transpiration T_{leaf}) wurde mit einem Porometer gemessen und physiologisch auf der Basis von Mikroklimadaten (photosynthetisch aktive Strahlung PAR für Lichtintensität, Temperatur, Sättigungsdefizit der Luft) und der Bodenfeuchtigkeit interpretiert. Die Wassernutzungseffizienz (WUE, als Quotient aus Photosynthese- CO_2 -Nettoaufnahme und Wasserabgabe durch Blatttranspiration) wurde verwendet, um die Bandbreite der Reaktion der Weidefläche und des Grases auf die Umgebungsvariablen der Untersuchungsfläche zu analysieren. PAR und das Sättigungsdefizit der Luft (VPD) erscheinen als bestimmende Faktoren für T_{leaf} und ET_{Sci} . Die WUE von *Setaria sphacelata* ist bei hohem VPD und gleichzeitig hoher Sonneneinstrahlung bei wolkenlosem Himmel besonders niedrig. Die mit dem Szintillometer gemessenen Verdunstungsraten (2.26 bis 4.96 $mm Tag^{-1}$) korrelieren sehr gut mit den mittels des Penman-Monteith Ansatz errechneten Werten für ET ($r^2 = 0.95$). Auch die mittels Porometer gemessene Blatttranspiration (0.83 bis 2.41 $mm Tag^{-1}$) zeigt einen guten, wenn auch statistisch schwächeren Zusammenhang mit ET_{Sci} ($r^2 = 0.78$). Die geringere Korrelation zwischen T_{leaf} und ET_{Sci} resultierte nicht aus einer Signalkontamination durch Luftmassenadvektion aus dem Einzugsbereich (fetch) des Szintillometer-Pfads. Die Überprüfung zeigte keine derartigen Effekte. Bodenwasserlimitierung der Verdunstung konnte ebenfalls ausgeschlossen werden. Da ET direkt vom Wasserdampfsättigungsdefizit der Luft abhängt, die Verdunstung durch die Blätter aber hauptsächlich durch die Stomata erfolgt, sind physiologische Prozesse in der Stomataregulation für die etwas geringere Korrelation von ET_{Sci} und T_{leaf} im Tagesverlauf verantwortlich.

Keywords: Evapotranspiration, transpiration, Setaria, pasture, tropical mountain, Andes, southern Ecuador

1 Introduction

Biodiversity and ecosystem services such as water and carbon regulation are affected by environmental changes such as land use and climate change (CARDINALE et al. 2012 and many more). This also holds true for the Andes of south-eastern Ecuador, which is the second hottest biodiversity hotspot on the planet. Here, natural forest is steadily being converted into agricultural land by the local population through slash and burn activities (KNOKE et al. 2014; THIES et al. 2014; CURATOLA FERNÁNDEZ et al. 2015). BUYTAERT et al. (2005) find that land use changes in the Andes of Ecuador lead to a deterioration of water regulation services. Proper water management practices are crucial to Ecuador because approximately 50 % of the nation's electricity is generated by hydroelectric power plants, the performance of which depends on a well-regulated hydrological system (PELÁEZ-SAMANIEGO et al. 2007). To properly assess the interplay between climate and land use changes, including the water and carbon cycles, BONAN (2008) emphasized the importance of improved land surface models (LSMs), including a proper parameterization and validation. The latter, however, requires the measurement of evapotranspiration (ET), CO₂ uptake and water use efficiency (WUE) for all relevant plant functional types, data that are hardly available for tropical ecosystems. While transpiration and WUE can be operationally measured at the leaf level using modern portable porometers, the observation of canopy ET still poses problems in remote areas and in complex terrain. Lysimeters cannot be installed on steeper mountain slopes, while the applicability of Eddy Covariance (EC) systems to retrieve the latent heat flux that serves as the basis of ET calculations needs comprehensive data corrections (for problems and required corrections refer to HAMMERLE et al. 2007; ETZOLD et al. 2010).

The recent introduction of a new laser-based ET scintillometer (ET_{sci}) makes it possible to derive ET_{sci} values integrated over a certain path length, thus providing statistically reliable measurements. Large aperture scintillometers (LAS), which operate at a wavelength of 850 nm, are usually used for path lengths between hundreds of meters and several kilometers (250 m–4 km). On the other hand, dual-beam surface laser scintillometers (SLS) operating at 670 nm are generally applicable to shorter path lengths (50–250 m) and thus more appropriate for applications of small extents. By

comparing methods for EC, SLS and Bowen ratio (BR) measurements over mesic grasslands, SAVAGE (2009) and SAVAGE et al. (2010) stressed that SLSs offer a particularly robust method for ET_{sci} assessments. By analyzing EC and SLS measurements, the relationship between fetch area and wind speed and direction played a measurable role in the variability of the derived quantities, such as sensible and latent heat flux (ODHIAMBO 2011), and should thus be included in SLS studies as well.

The aim of this paper is to combine transpiration (T_{leaf}) and photosynthesis (P_{leaf}) measurements at the leaf level with ET_{sci} observations at the canopy level for a homogeneous pasture in the Andean mountains in order to analyze the relation of water fluxes at the soil-vegetation-atmosphere boundary and biomass production during different weather conditions. Furthermore, the comparison of T_{leaf} and ET_{sci} should help to assess the applicability of SLS measurements in high mountain areas.

2 Methods

2.1 Study site

Measurements were carried out between 12 and 19 November 2013 on a pasture site close to the ECSF research station in the San Francisco River Valley in the Andes of SE Ecuador (refer to BENDIX and BECK 2009). The natural mountain rain forest in this area generally reaches an altitude of 3000 m a.s.l. However, wide areas of the forest have been cleared for pasture farming. The pasture grass *Setaria sphacelata* is the most common species planted in the mid-range, between 1500 and 2600 m a.s.l. The study area has a humid climate year-round, with an average annual rainfall close to 2200 mm (BENDIX et al. 2008). It is characterized by one marked rainy season (Mar–Aug) and a period with slightly reduced rainfall (Oct–Dec) (ROLLENBECK and BENDIX 2011). Average air temperature is 15.5 °C (ECSF meteorological station), with only small fluctuations over the year (BENDIX et al. 2008). Besides the synoptic wind, which is dominated by the tropical easterlies (ROLLENBECK and BENDIX 2011), wind circulation in the lower valley is characterized by the mountain breeze system with upslope and up-valley winds during the day and nocturnal katabatic downslope and down-valley cold air drainage flows (BENDIX et al. 2008; MAKOWSKI GIANNONI et al. 2013).

2.2 Measurements of transpiration and evapotranspiration

Figure 1 and table 1 show the experimental set up. In order to compare leaf transpiration (T_{leaf}) and canopy evapotranspiration (ET_{Sci}), a portable photosynthesis system (LiCor LI6400XT, LiCor Inc., Lincoln, NE, USA) and a surface laser scintillometer (SLS) (Scintec SLS40 with evapotranspiration extension, Scintec AG, Rottenburg) were used. The SLS is an optical instrument which uses the covariance in a dual-beam laser (at 670 nm wavelength) to estimate atmospheric turbulence, heat and momentum flux. Combined with an automatic weather station AWS_{Sci} , the SLS is used to estimate ET_{Sci} by completing the energy balance using the Monin-Obukhov similarity theory (MOST). A review of the SLS, including a description of the algorithm, is given in ODHIAMBO and SAVAGE (2009). The automatic weather station (AWS_{Sci}), installed at the SLS receiver, measured net radiation, soil heat flux, air temperature, and relative humidity. The AWS_{Sci} data were used to estimate both ET_{Sci} and water vapor flux using the Penman-Monteith (T_{PM}) equation (section 2.3). Since the AWS_{Sci} cannot measure wind or soil moisture profiles, we used data from an AWS_{Burn} situated 450 meters (horizontal distance) away from the scintillometer path (refer to SILVA et al. 2012). The SLS was installed two

meters aboveground and with a path length of 89 meters in relatively flat terrain. The SLS propagation path stretched over a closed canopy (100 % cover) of the pasture grass *Setaria sphacelata* (average plant height of 0.53 meters). Within a horizontal radius of about 300 meters, the terrain rises from 1750 to 2000 meters with slopes between 1° and 66° (31° on average). Secondary vegetation, mainly bracken fern and shrubs, as well as afforestation with *Pinus patula*, surround the pasture on which the measurements were taken. Observations were performed over the course of eight days under both sunny and cloudy conditions. Data from three days had to be discarded due to bias introduced by scattered rain showers. Thus, five days' worth of data recorded in ten-minute intervals were analyzed.

Leaf transpiration and net CO_2 uptake rates were measured on mature green leaves of various *Setaria sphacelata* tufts. Each day a different tuft along the scintillometer path was selected at random. Mature leaves of *Setaria sphacelata* tufts are considered physiologically similar and thus equally responding to atmospheric forcing. Because *Setaria* pastures are planted manually, the tufts of one pasture are of the same age. Previous measurements on three of the tufts showed similar rates of maximum photosynthetic net CO_2 uptake, which differed by no more than 12 % among each other. The sensor head of

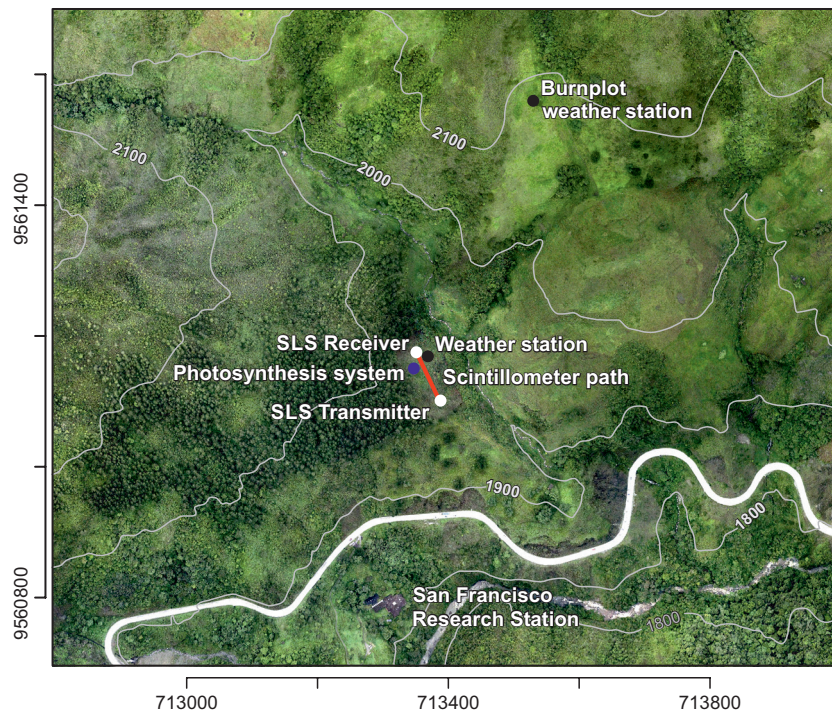


Fig. 1: The study site and the localization of the experimental setup in the valley of the San Francisco River in Southern Ecuador

the portable photosynthesis system (LI-6400XT, LiCor Inc., Lincoln, NE, USA) was positioned so as to keep the leaf in its natural position as much as possible. Ambient conditions were maintained in the cuvette chamber. For establishing a light response curve of photosynthetic net CO₂ uptake, an external light source (6400-02B LED light source, LiCor Inc., Lincoln, NE, USA) was mounted to the cuvette chamber and measurements were performed when CO₂ uptake was stable after adapting to the different light steps. Consistently with SLS, AWS_{Sci}, and AWS_{Burn} data, porometer data recorded in ten minutes were used for further analysis.

Water use efficiency (WUE) is calculated using the porometer data according to FARQUHAR et al. (1989) (Tab. 1):

$$WUE = \frac{P_{Leaf}}{T_{Leaf}} \quad [\mu\text{mol}/\text{mmol}] \quad (1)$$

Spatial data for the area adjacent to the scintillometer path was used for ancillary analyses. This includes a digital elevation model (DEM) and the canopy height derived from the land surface model (DSM) of a laser scanning campaign conducted in the San Francisco River Valley (SILVA and BENDIX 2014).

2.3 Applicability of the methods

Two main conditions are required to apply the Monin-Obukhov similarity, which must be met for measuring ET_{Sci} in mountain terrain. First, despite the pasture's location in such terrain, the short SLS

path length allows us to find a suitable flat terrain with homogenous vegetation. Second, the propagation path length is set two meters above ground, which is more than twice as high as the vegetation cover (average 0.53 meters height), providing high sensitivity without signal saturation at strong turbulences. An estimation of the fetch showed high homogeneity on the pasture area up to around 100 meters away from the propagation path. Field and aerial photo observations confirmed this appreciation. In addition, even if homogeneity would not be fully satisfied, the similarity theory is still valid for a limited range of the ratio between the measurement height and the Obukhov length (z/L) (MORAES et al. 2005; MARTINS et al. 2009). Finally, as the condition of a homogeneous green vegetation cover is met, single point measurements of T_{leaf} could be used as a basis for upscaling transpiration (and photosynthetic net CO₂ uptake) from the leaf level to the canopy of the measuring path of the ET_{Sci} measurements. That is the rationale behind the simultaneous use of the porometer and the scintillometer.

In the current study area, the above mentioned preconditions for MOST are as far as possible adhered, which can be verified in the measurements. With the propagation path of 89 meters good SLS-signal sensitivity and no saturation at strong turbulences in sensible heat flux are confirmed by the distribution of the inner scale of the refractive index fluctuation (mean = 7.5 and range [0.75, 18.82]). The inner scale of the refractive index fluctuation – measured by the SLS – is the smallest diameter of the occurring eddies and should have a lower limit of 2 mm, which in our case holds for 97 % of the data. In addition, according to MORAES et al. 2005, the

Tab. 1: Variables and field instrumentation

Variable	Instrumentation	Model / Company
Leaf Transpiration (T _{leaf})	Portable porometer	LI-6400XT (LiCor Inc., Lincoln, NB, USA)
Leaf net CO ₂ uptake (P _{leaf})		
Canopy Evapotranspiration (ET _{Sci})	Scintillometer + AWS _{Sci}	SLS-40 (Scintec AG, Rottenburg a.N., Germany)
Friction velocity		
Net radiation	Scintillometer-AWS (AWS _{Sci}) Pyrradiometer	8111 (Schenk GmbH, Austria)
Soil heat flux	Heat flux plate	HFP01 (Campbell Sci., USA)
Temperature & Rel. humidity	Thermometer and hygrometer	HC2S3 (Campbell Sci., USA)
Precipitation	Rain gauge	52203 (RM Young, USA)
Wind speed & direction	Burnplot-AWS (AWS _{Burn}) Ultrasonic anemometer	WindSonic (Gill, Inc. UK)
Soil moisture	Soil moisture sensor	10HS Decagon devices, USA)

standard deviation of wind speed normalized by the friction velocity indicates in terms of z/L where turbulence has been properly measured. A breakdown of MOST could have occurred under very stable ($z/L > 0.5$) or very unstable ($z/L < 0.5$) atmospheric conditions. Though, we observed a typical behavior for $-0.5 < z/L < 0.5$, which occurred in 93 % of the data. Last, because scintillometer-based observations may be biased by fetch effects of the adjacent area, it is necessary to run a fetch contribution analysis to guarantee that the results presented for the ET_{Sci}/T_{leaf} relationship are not severely affected by ET processes from outside the *Setaria* pasture (please refer to section 3.3).

2.4 Ancillary data processing

To assess the feasibility of the SLS observations, our first step was to compare the measurements with calculations of T_{PM} based on the Penman-Monteith (PM) model. In our case, T_{PM} closely represents ET, mainly because of two reasons. First, the pasture grass completely covers and thus shades the ground, thus minimizing bare soil evaporation. Second, SLS measurements are from precipitation-free days solely, thus minimizing the evaporation of canopy intercepted water. Sub-hourly PM calculations require proper parameterization (for the required equations and parameters the reader may refer to McMAHON et al. 2013). Unlike in McMAHON et al., the aerodynamic and surface resistance calculations r_a and r_s are provided by BONAN (2008), which is important for the sub-hourly applications used in this paper:

$$r_a = \frac{\ln \left[\frac{z_m - d}{z_{om}} - \psi_m(\zeta) \right] \cdot \ln \left[\frac{z_h - d}{z_{oh}} - \psi_h(\zeta) \right]}{k^2 u_z} \quad (2)$$

in which z_m is the height of the laser beam (m), z_b is the height of the temperature/humidity instrument (m), d is the zero plane displacement height (m) derived from plant height in the path using the DSM, z_{om} the roughness length of momentum (m), z_{oh} the roughness length of heat and vapor transfer (m), k is the von Karman constant, and u_z the wind speed ($m s^{-1}$). The SLS provides the friction velocity (u_s), which according to OKE (2002), is proportional to the square of the wind speed (u_z). The terms $\psi_m(\zeta)$ and $\psi_h(\zeta)$ are for stability correction for momentum and heat, respectively. These terms are calculated using scintillometer-based values of sensible heat flux

and, according to BONAN (2008), are given for unstable conditions ($\zeta < 0$) by:

$$\psi_m(\zeta) = 2 \ln \left[\frac{1+x}{2} \right] + \ln \left[\frac{1+x^2}{2} \right] - 2 \tan^{-1} x + \pi/2 \quad (3)$$

$$\psi_h(\zeta) = 2 \ln \left[\frac{1+x^2}{2} \right] \quad (4)$$

$$x = (1 - 16\zeta)^{1/4} \quad (5)$$

and for stable conditions ($\zeta > 0$) by:

$$\psi_m(\zeta) = \psi_h(\zeta) = -5\zeta \quad (6)$$

in which $\zeta = (z-d)/L$, z is set the measurement height (z_m), and L is the stability length, which is calculated based on scintillometer values of sensible heat flux, as given by:

$$L = - \left(u_s^3 T \rho C_p \right) / (kgH) \quad (7)$$

in which u_s is the friction velocity, k is the von Karman constant (0.41), g is the acceleration due to gravity ($9.81 m s^{-2}$), T is the air temperature (K), H is the sensible heat flux ($W m^{-2}$), ρ is the density of the air ($kg m^{-3}$), and C_p is the heat capacity of the air.

The stability length (L), and thus the sensible heat flux (H), are obtained directly from the SLS measurements by the numerical iteration of L and H dependent functions, which in turn are dependent on the fluctuations in the refractive index of the air, measured by the laser beam of the SLS. The semi-empirical MOST similarity functions applied in this case are from THIERMANN and GRASSL (1992) and also reviewed in ODHIAMBO and SAVAGE (2009). The surface resistance is given by:

$$r_s = \frac{r_l}{LAI_{active}} \quad (8)$$

in which r_l is the stomatal resistance of a single leaf (s/m) which is obtained from the porometer measurements in the scintillometer path, and LAI_{active} is the photosynthetic active leaf area index (m^2/m^2), or the sunlit (green) LAI, as derived by BENDIX et al. (2010) for *Setaria sphacelata*. The LAI of *Setaria* was obtained in the field using the light transmittance method (LAI-2000, LiCOR, Lincoln, NE, USA), and the sunlit LAI, or the LAI_{active} , equals 77 % of LAI. The sunlit fraction of LAI considers leaf area and inclination at hemispherical illumination (BENDIX et al. 2010). In addition, both LAI and sunlit LAI fractions were applied in computer simulations, which

were validated by the yield (net CO₂ uptake and annual biomass production) of the forage grass *Setaria* (SILVA et al. 2012).

The fetch area for the SLS was calculated for the wind direction and wind speed of each time step according to HSIEH et al. (2000). The weighted sum of the canopy height was used as the spatial variable to indicate vegetation type within the fetch area to explain ET for each wind sector. The fetch calculation requires the wind speed in the scintillometer path, which is not provided by the AWS_{Sci}. The AWS_{Sci} does provide a friction velocity measurement, however, which is related to wind speed. We conducted a regression analysis between friction velocity from AWS_{Sci} and wind speed from AWS_{Burn} to calculate the wind speed in the scintillometer path with the derived regression equation ($r^2 = 0.73$, slope = 0.177).

3 Results and Discussion

3.1 Feasibility of ET measurements with the scintillometer

In a first step, the ET_{Sci} measured with the scintillometer was compared to T_{PM} calculations in order to assess the feasibility of the instrument. Figure 2 shows ET_{Sci} and T_{PM} together with leaf transpiration as well as rainfall and soil water in the course of a week. We found very good general consistency between scintillometer ET_{Sci} observations and T_{leaf} calculations (T_{PM}) with the Penman-Monteith (PM) approach adapted to *Setaria* pastures

for every day. However, peak T_{PM} at noon is higher than ET_{Sci} on sunny days (Fig. 2, left). Other studies in which lysimeters were used to determine ET (e.g. LOPEZ-URREA et al. 2006) have shown that PM calculations slightly overestimate ET. The correlation (Fig. 2 right) between both methods is nevertheless strong and in the same range of lysimeter studies (r^2 of 0.92 in LOPEZ-URREA et al. 2006). While data pairs largely coincide with the one-by-one line up to an ET of 0.6 mm h⁻¹, the correlation becomes less strong and scatter clearly increases above that value. In particular, days with intermittent cloudy and sunny periods seem to deliver lower T_{PM} values, while ET_{Sci} peaks seem to be lower on more sunny days.

3.2 ET, T and WUE of the *Setaria* pasture under different weather conditions

Figure 3 presents the detailed daily courses of transpiration (T_{leaf}), evapotranspiration (ET_{Sci}), photosynthesis (P_{leaf}) and atmospheric variables to show the situation on three exemplary days: one with intermittent sunny and cloudy weather (12 Nov), one that is entirely overcast (15 Nov) and one that is entirely sunny (19 Nov).

On the day with intermittent cloudiness (Fig 3 a, d, g), photosynthesis and transpiration generally increased until noon, with a clear relation to corresponding peaks in PAR and between T_{leaf} and P_{leaf}. After 13:00 LST, PAR and transpiration continued to increase while photosynthesis began to decline

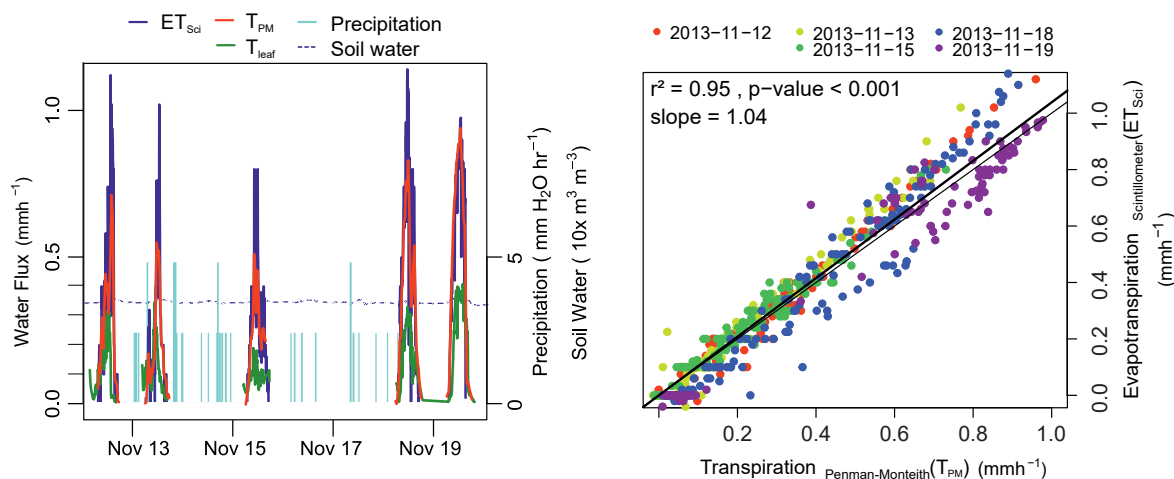


Fig. 2: (Left) Comparison of daily courses of ET_{Sci} (blue), T_{PM} (red) and T_{leaf} (green) together with precipitation (light blue) and soil water (dashed blue) on a *Setaria sphacelata* pasture in the course of a week. (Right) Relation between T_{PM} and ET_{Sci}. Colors indicate day of measurement. Bold slope line in black is the regression line for all days. The thin line shows the one to one line. In the PM-Model, a photosynthetically active LAI of 2.5 is used

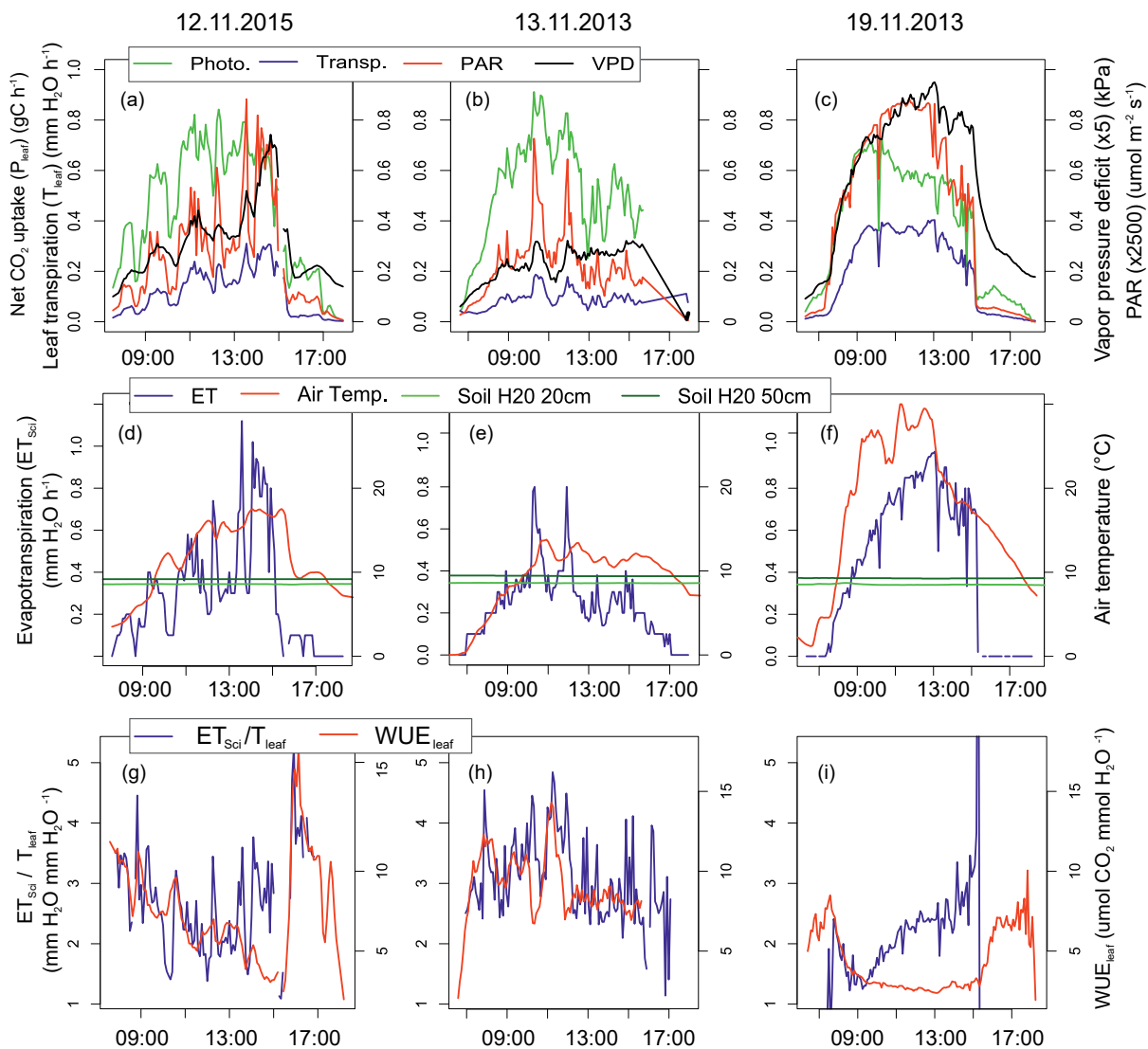


Fig. 3: Courses of transpiration (T_{leaf}), evapotranspiration (ET_{Sci}), photosynthetically net CO_2 uptake (P_{leaf}) and atmospheric variables (PAR, VPD, Soil water and air temperature) for three days. P_{leaf} is converted to gC using the relation $1 \mu\text{mol m}^{-2}\text{s}^{-1} = 0.0432 \text{ gC m}^{-2}\text{h}^{-1}$. T_{leaf} is converted to $\text{mm H}_2\text{O}$ using the relation $1 \text{mol m}^{-2}\text{s}^{-1} = 0.0648 \text{ mm m}^{-2}\text{h}^{-1}$

slightly. All values immediately dropped after 15:30 LST, when the study site became shaded. ET_{Sci} generally followed the course of T_{leaf} and the relations between ET_{Sci} and T_{leaf} increased with peaks in PAR (here taken as a proxy for the amount of global radiation). This reflects an enhanced portion of evaporation (E) in ET_{Sci} during periods of high insolation. It also holds for the average level of $ET_{\text{Sci}}/T_{\text{leaf}}$ after 13:00 LST, which is somewhat higher in its mean value than before noon due to a slight decrease of stomatal conductance as indicated by the decrease of the rate of photosynthetic net CO_2 uptake. It is important to note that oscillations in $ET_{\text{Sci}}/T_{\text{leaf}}$ mainly reflect the dependence of

ET_{Sci} and T_{leaf} on the available energy. This variable strongly depends on solar radiation, which varied within minutes on cloudy days due to illumination geometry. In addition, while T_{leaf} is the primary outcome of stomata regulation, ET_{Sci} values include all sources of evaporation. Further, WUE generally decreased to very low values ($< 5 \mu\text{mol CO}_2 \text{ mmol H}_2\text{O}^{-1}$) as the day progressed, while peak values were observed during phases of cloud cover in the morning and again in the late afternoon. The same principal relations hold for the cloudy day (Fig. 3 b, e, h), on which WUE is relatively constant from sunrise until sunset and comparatively high at approximately $8 \mu\text{mol CO}_2 \text{ mmol}^{-1} \text{ H}_2\text{O}$.

The entirely sunny day reveals the most homogeneous situation (Fig. 3 c, f, i). PAR and ET show a similar daily course, while photosynthesis decreases after 11:00 LST due to stomatal limitation indicated by T_{leaf} values remaining nearly constant at about 0.4 mm h^{-1} throughout the entire period of strong irradiance. The steady increase in the $ET_{\text{Sci}}/T_{\text{leaf}}$ ratio clearly shows the increasing portion of E in ET_{Sci} as the day progresses. From 8:30 to 10:30 LST, photosynthesis remains constant, while transpiration continues to increase until 9:30 LST. This results in a dramatic decline of WUE, which reaches a minimum level of around $2 \mu\text{mol CO}_2 \text{ mmol H}_2\text{O}^{-1}$ from 9:00 until 15:30 LST. Once the area becomes shaded in the late afternoon, WUE increases again to values between 7 and $8 \mu\text{mol CO}_2 \text{ mmol H}_2\text{O}^{-1}$ as transpiration steadily decreases and photosynthesis shows a transitory positive response to PAR. It is obvious that photosynthetic net CO_2 uptake (P_{leaf}) as well as T_{leaf} were limited, although soil moisture at different depths (Fig. 3d-f) remained high throughout the entire day, not indicating soil induced drought stress. However, figure 3 (top and bottom) shows an inverse relationship between photosynthesis and vapor pressure deficit (VPD), most obvious at the peak levels of the saturation deficit (12 and 19 Nov). T_{leaf} does not reflect this because at a given stomatal conductance, transpiration is a function of VPD and thus increases as the saturation deficit increases, while photosynthesis responds to PAR under these conditions. On the cloudy days (13 and 15 Nov) VPD did not show great diurnal fluctuations and transpiration remained rather low (Fig. 3 b). C4 plants such as *Setaria* are known for high biomass production at high light intensities, high temperatures and limited moisture (see e.g. KADEREIT et al. 2014).

The light (PAR) response curve for *Setaria sphacelata* saturates at $1000\text{--}1250 \mu\text{mol m}^{-2} \text{ s}^{-1}$. The maximum net CO_2 uptake equals $15.02 \mu\text{mol CO}_2 \text{ m}^{-2} \text{ s}^{-1}$ (standard deviation = 1.8) taking six samples on three leaves. Therefore, irradiation above that intensity cannot increase photosynthetic net

CO_2 uptake. Because T_{leaf} remained constant between 9:30 and 13:00 LST as VPD increased on the sunny day, stomatal conductance must have decreased, which explains the decrease in photosynthetic net CO_2 uptake during midday. Likewise, the highest photosynthetic rates on this day must have been curtailed by stomatal conductance. This interpretation explains the higher peak rates of photosynthetic net CO_2 uptake during spells of higher PAR on the overcast or partly sunny days (12 and 15 Nov) when VPD was low. Another point worth mentioning in that respect is air temperature (refer to SILVA et al. 2013). Temperatures below 20°C (12 and 15 Nov) are clearly suboptimal for a C4-grass. Thus, under an optimal combination of PAR, VPD, and temperature, even higher photosynthetic rates could be expected. Due to weather conditions, however, this is unlikely in the immediate research area but might occur at lower elevations in the San Francisco River Valley.

A correlation matrix corroborates the interpretation's findings (Tab. 2). Photosynthesis (P) shows a moderately positive correlation to PAR, air temperature and transpiration. Transpiration (T) shows a markedly stronger positive correlation to PAR and air temperature in particular. On the other hand, WUE is inversely related to PAR. Also, air temperature and VPD show negative influence on WUE. PAR is considered a proxy for the total radiation.

Figure 4 summarizes the results and shows that the $ET_{\text{Sci}}/T_{\text{leaf}}$ ratio is in the range of 2.49, with higher values (lower T_{leaf}) during cloudy days with a low VPD. The results generally agree with those from similar studies. For instance, YEPEZ et al. (2005) found ET/T ratios between 2.33 and 2.86 with isotope studies in grasslands with *Eragrostis lehmanniana*. For high elevation grassland systems in Mongolia, HU et al. (2009) observed ratios ranging between 1.3 and 2.6 for the growing season in four communities dominated by *Leymus chinensis*, *Agropyron cristatum*, *Cleistogenes squarrosa* and *Carex*

Tab. 2: Correlation matrix between atmospheric forcing and plant response variables for the three days displayed in figure 4 (6:00–18:00)

	P_{leaf}	T_{leaf}	Temperature	VPD	PAR	WUE
P_{leaf}	1.00					
T_{leaf}	0.68	1.00				
Temperature	0.63	0.90	1.00			
VPD	0.45	0.88	0.96	1.00		
PAR	0.69	0.94	0.86	0.82	1.00	
WUE	0.02	-0.55	-0.44	-0.55	-0.44	1.00

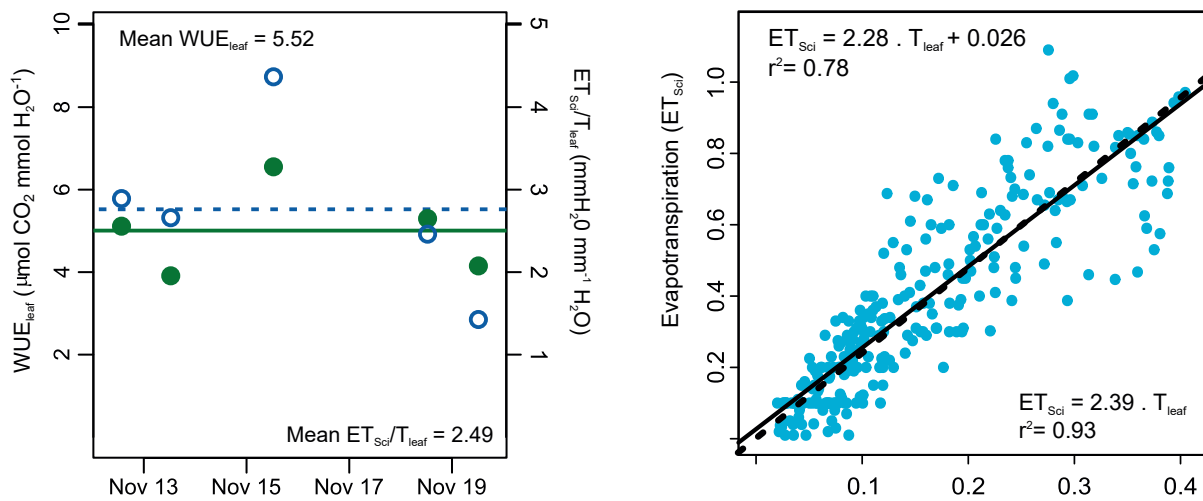


Fig. 4: (left) Average daily relationship between ET_{Sci} and T_{leaf} (green) and WUE (blue) for the Setaria pasture. (Right) Relationship between ET_{Sci} and T_{leaf} using the 10-minute data

duriuscula, respectively. WUE turned out to be high for the *Setaria sphacelata* pasture under cloudy conditions ($WUE = 8.74$). The average value of 5.52 is also in accordance with other studies. For *Setaria viridis*, LUO et al. (2009) found WUE values between 4.77 and 5.30 $\mu\text{mol CO}_2 \text{ mmol}^{-1} \text{ H}_2\text{O}$ under unstressed conditions, which decrease to values around 1.65 $\mu\text{mol CO}_2 \text{ mmol}^{-1} \text{ H}_2\text{O}$ under severe drought stress. In laboratory experiments with *Setaria sphacelata*, a reduction of WUE from 10 to approximately 2 $\mu\text{mol CO}_2 \text{ mmol}^{-1} \text{ H}_2\text{O}$ was reported under upcoming drought stress at a relative leaf water content of around 65% (DA SILVA and ARRABACA 2004). Although significant water stress inhibited metabolic activity in the mesophyll, stomatal limitation of CO_2 diffusion was the main reason for a decrease in photosynthesis (DA SILVA and ARRABACA 2004). The average WUE of around 5.52 found in our experiment shows this limitation also to occur naturally. Finally, figure 4 (right) corroborates the good ratio of canopy-level ET_{Sci} and leaf-level T_{leaf} ($r^2 = 0.78$). This relation shows that ET_{Sci} is significantly controlled by T_{leaf} and less influenced by evaporation from other sources than the leaves.

3.3 Potential dependence of ET measurements on fetch area characteristics

Wind speed in the valley during the study period was low, with a mean wind speed of 1.43 m s^{-1} ($\sigma = 0.46$), with 69% of data below this average (Fig. 5, left). As pointed in section 2.4, low wind speed leads to a relative small fetch area. Winds

predominantly blow from the eastern to south-eastern sector, resulting (i) from the prevailing easterlies as synoptic forcing (ROLLENBECK and BENDIX 2011) which are channelized by the valley's E-W orientation, and (ii) the thermally induced up-valley breeze during the daylight period (BENDIX et al. 2008, 2009) in the same direction. While a constant direction around 125–130° prevails during daylight hours on the overcast and partially sunny days (12–15 Nov), the days with more sun (especially 19 November) show a clear thermally induced breeze cycle from nocturnal downslope and down-valley cold air drainage flow to upslope and up-valley winds during the day (Fig. 5, right).

The aerial photo in figure 6 (left) shows the footprint areas which are covered by different functional vegetation types. The cover in the E sector mainly consists of *Setaria* pastures and smaller shrubs; the ESE sector exclusively encompasses pasture area. The surface of the S, SW and NNE sectors include *Setaria* pastures and afforestation with *Pinus patula*. By distance weighting of the relative contribution to the SLS signal, the example for the eastern wind direction (Fig. 6, right) clearly shows that the signal is derived almost entirely from the *Setaria* pasture in the scintillometer path and very close adjacent areas.

Figure 7 reveals the contributing wind sector for each ET_{Sci} signal and the contributing vegetation type, indicated by vegetation height. The result does not support a clear correlation between the measured ET_{Sci} and land cover. For most of the wind sectors, ET_{Sci} spans the entire ET_{Sci} range measured for the pasture (canopy height < 2 m).

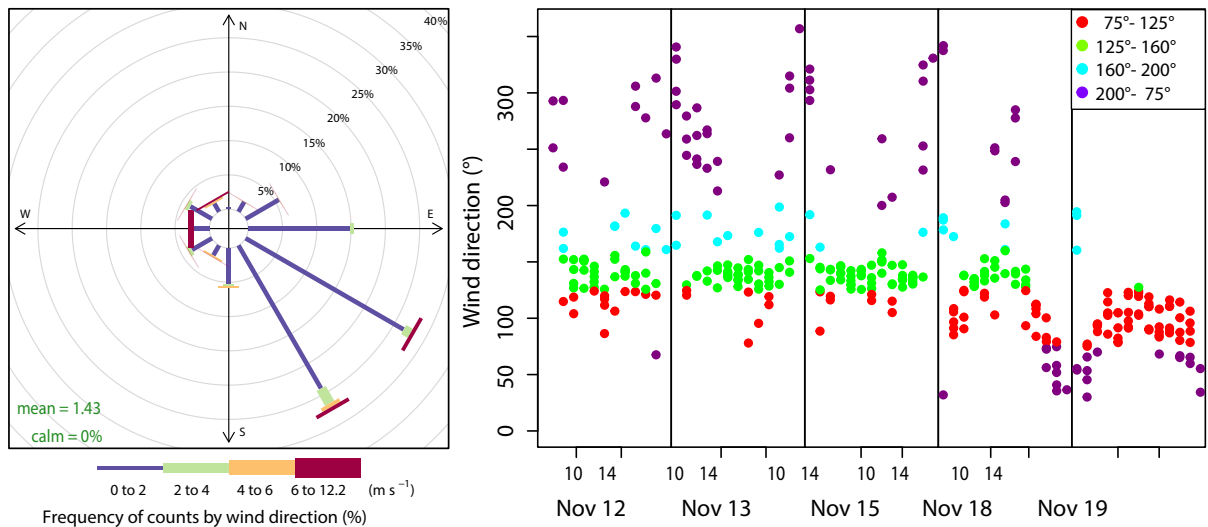


Fig. 5: (left) Frequency of wind direction, (right) diurnal course of wind direction for selected days (colors indicate the fetch area sectors as presented in figure 6 left)

Only ET measurements during wind sectors facing the *Pinus* plantation (canopy height > 4 m) were lower. However, these ET observations are clearly related to the early morning and late afternoon hours, when ET_{Sci} and T_{leaf} were attenuated due to reduced radiative forcing (Fig. 3). Thus, any dominating influence the fetch area has on the observed ET_{Sci}/T_{leaf} ratios was excluded for the study period.

3.4 ET measurements and the context of the conversion of forest to pasture

Table 3 presents a summary of measurements together with representative meteorological variables. As expected, the variables total ET_{Sci} ($mm\ day^{-1}$) and total T_{leaf} ($mm\ day^{-1}$) show a good agreement with available energy ($mm\ day^{-1}$). At the same time, photo-

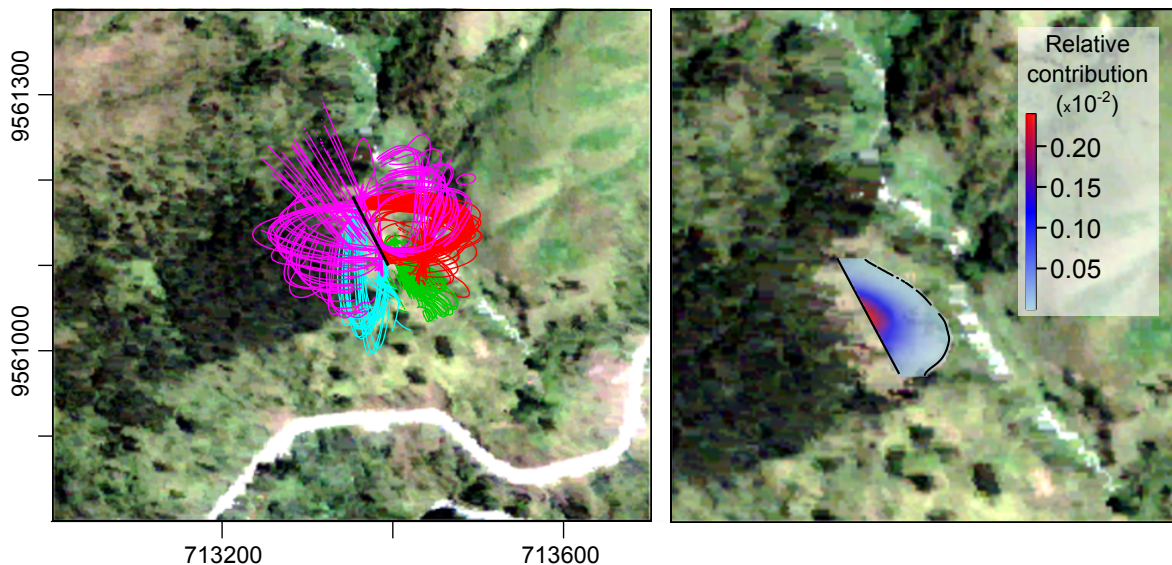


Fig 6: Footprint contribution for the study period around the scintillometer path (black line in both figures): (left) all footprints (constraining line at 75 % of influence) in ten minutes time-steps, (right) contribution function for the average wind speed of 1.43 $m\ s^{-1}$ and wind direction of 90°. The average slope in the footprint of the scintillometer measurements is in 29.6 in average. According to land use classifications of the area (GÖTTLICHER et al. 2009; CURATOLA FERNÁNDEZ et al. 2013), bright greenish colors indicate active pastures, brownish colors bracken fern and shrub successions and dark green colors forest and afforestation patches

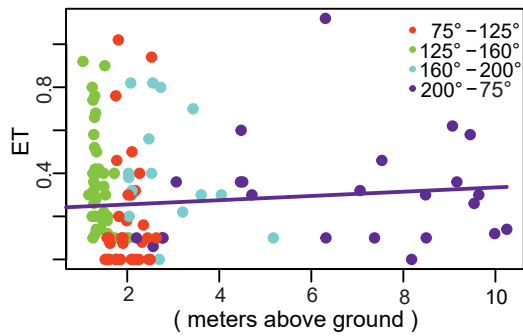


Fig. 7: Scatterplot of the spatial variable canopy height of the fetch area and its close surroundings related to the ET observations during prevailing wind sector classes

synthetically net CO_2 uptake (P_{leaf}) (gC day^{-1}) remains nearly constant along the week, with a slight tendency towards higher values on days with overcast and scattered clouds (15 and 18 Nov). Photosynthetic gas exchange is controlled by both light intensity and the conductivity of the stomata. The latter is controlled by the water status of the leaves and the atmospheric water vapor deficit. Therefore it is not surprising that the available energy does not necessarily directly correspond with net CO_2 uptake, while evapotranspiration strongly depends on the available energy and atmospheric conditions. For comparison with the literature, we used a weighted calculation to obtain annual ET_{Sci} considering typical cloud conditions. First, the minimum and the highest values of table 3 are multiplied by the fraction of 0.88 overcast days per year (BENDIX et al. 2008) and by the remaining of 0.22 sunny days per year, respectively. Then, the sum of these terms is multiplied by 365 to yield a typical annual ET_{Sci} of $1124 \text{ mm year}^{-1}$. This value is in good agreement with model-based values found for low-intensity grazed pasture in our study area (WINDHORST et al. 2014). In addition, similar obser-

vations have been made for the tropical cloud forest (BRUIJNZEEL et al. 2011). An ET of $1281 \text{ mm year}^{-1}$ was found in a forested micro-catchment nearby our study area (FLEISCHBEIN et al. 2011). In the forest, low VPD and high fog-intensity seems to lower ET, while the opposite is expected on the areas converted into pastures (KNOKE et al. 2014). On less intensively used pasture, higher ET is associated with a larger infiltration and larger base flow, while radiation limits ET and high near-surface lateral flow is expected in the forest (WINDHORST et al. 2014). BRUIJNZEEL et al. 2011 reported that the quick runoff response of intensively used pastures at local scale could not be observed at operational catchment scale. Based on the present ET measurements, less intensively used pastures should counterbalance both, base flow and lateral flow at catchment scale due to relative high ET values under sufficient water supply (i.e. almost constant soil water content).

4 Conclusions

In this case study from the SE-Ecuadorian Andes, we investigate the relationship between canopy-level evapotranspiration and leaf-level transpiration and photosynthesis to better understand the plant component of the water and carbon cycles of a high Andean pasture dominated by the C4 grass *Setaria sphacelata* during various typical weather conditions. The new methodological combination of a laser scintillometer and a porometer revealed a strong relationship between canopy ET, or ET_{Sci} , and leaf transpiration (T_{leaf}) for a *Setaria sphacelata* pasture, nearly undisturbed by fetch effects of the surrounding terrain. However, slight deviations on the relation between ET_{Sci} and T_{leaf} , in particular at higher

Tab. 3: Summary of water flux (ET_{Sci} , T_{leaf}), net photosynthetic CO_2 uptake (P_{leaf}) converted to gC per day, heat flux (H_{Sci}), PAR radiation, and total net radiation for the five days of measurements (November 12–19 2013). Available energy is the daily net total radiation converted to water depth (mm) using the relation $1 \text{ MJ m}^{-2} = 0.408 \text{ mm}$. Midday averages are from observations between 11:00 and 14:00 for each day

Day Cloud condition	Nov 12 broken	Nov 13 broken	Nov 15 overcast	Nov 18 scattered	Nov 19 sunny	Average
Daily total ET_{Sci} (mm day^{-1})	3.00	2.26	2.69	4.48	4.96	3.48
Available energy (mm day^{-1})	3.40	2.72	3.11	5.65	6.29	4.23
Daily total T_{leaf} (mm day^{-1})	1.19	1.17	0.83	1.71	2.41	1.46
Daily total P_{leaf} (gC day^{-1})	4.59	4.13	4.81	5.59	4.57	3.40
Midday PAR (W m^{-2})	282.80	199.62	105.96	216.31	412.40	243.42
Midday ET_{Sci} (W m^{-2})	285.95	331.90	178.29	334.49	574.87	341.10
Midday H_{Sci} (W m^{-2})	41.93	47.92	21.32	68.01	131.16	62.07
Midday net radiation (W m^{-2})	336.64	391.74	209.52	413.22	729.24	416.07
Midday Bowen Ratio	0.15	0.14	0.12	0.20	0.23	0.18

values, remain, as shown by the scatter in figure 4 (right), which summarizes all different (cloudy, partly overcast, sunny) days. This might have resulted from varying shares of leaf transpiration to ET, since evaporation directly depends on the incoming energy and the associated water vapor deficit while transpiration of a plant leaf is regulated by a multitude of factors, the most important being VPD and light intensity. Tropical C4 grasses were proven to regulate stomata conductance (and thus transpiration) very subtle under general good soil water conditions (LUDLOW et al. 1985). Environmental factors (light intensity and VPD) affect transpiration not quite independently, but the stomata control by a high VPD will always thwart control by light. Therefore a characteristic dependence of evaporation on VPD will be linear over a wide range whereas the corresponding relation of T_{leaf} and VPD shows an early saturation (Fig. 3c). As control of gas exchange is accomplished via the stomata conductivity, VPD also affects photosynthetic net CO_2 uptake in a similar way as T_{leaf} , however, the influence of the light intensity on photosynthesis is, at least at low to moderate VPDs stronger as that of the VPD (Figs. 3a and b). Whereas in general T_{leaf} appears to account for the bulk of ET, its share decreases with high VPDs. This could explain the stronger scatter of the data at high VPD (high ET). Thus, a temporal transient uncoupling of transpiration and evaporation especially in the afternoon cannot be completely ruled out. Regarding the latter, methodological issues must be considered as well, mainly the applicability of the similarity theory. In our study, a possible breakdown of the MOST theory in the measurement, due to the terrain configuration, did not impose a problem to the validity of the method. In more than 90 % of the data turbulence characteristics was observed to be well represented. A second methodological aspect that confirms this observation is the comparison of path-integrated SLS values with point porometer measurements of individual, randomly selected grass tufts along the path. Although the *Setaria* tufts showed low variability in their maximum rates of photosynthesis, some uncertainty must be implied in the intercomparison. For instance, the evaporation from plant surfaces because of nocturnal rain showers and dew-fall could also have contributed to the decrease in the share of leaf transpiration to ET. In light of these uncertainties by considering all different days together (Fig. 4 left), the relatively high coefficient of determination ($r^2 = 0.78$) between ET_{Sci} and T_{leaf} encourages the application of SLS instruments in tropical mountains. Last, coupling the relationship between

plant water and carbon by calculating WUE could be accomplished with porometer data. The question remains, how this information could be up-scaled to the scintillometer scale or beyond if, for instance, satellite data would allow us to derive instantaneous transpiration and CO_2 assimilation (equation 1). One approach to be considered is by using the ET_{Sci} to T_{leaf} relationship found in this study as a basis for the above mentioned upscaling. In this case, the spatial heterogeneity of the active leaf area and canopy interception should be considered. Indeed, some remote sensing techniques and approaches calculate WUE as the product of satellite-derived gross primary production and ET (or latent heat flux) (e.g. LU and ZHUANG 2010). If this needs to be done in a high temporal resolution (e.g. hourly intervals) our analysis shows that decoupling T and photosynthesis depends on the daily course of VPD and the change in the ET/T ratio might introduce uncertainties by replacing T in equation (1) with ET.

Acknowledgements

This study was completed as part of the program PAK823-825 ‘Platform for Biodiversity and Ecosystem Monitoring and Research in South Ecuador’, subprojects C5 and C6 (BE473/42-1 and BE1780/38-1). We are grateful to the German Research Foundation (DFG) for generously funding the project, to the Ecuadorian Ministry of the Environment (MAE) for the research permission and to the NCI foundation for logistic support. We thank Jörg Zeillinger, for local coordinator in the study area. We thank Paulina Alava-Nunes, for discussion about the plausibility of the ET values. We thank the anonymous reviewers for valuable comments on an earlier draft of this article.

References

- BENDIX, J. and BECK, E. (2009): Spatial aspects of ecosystem research in a biodiversity hot spot of southern Ecuador – an introduction. In: *Erdkunde* 63, 305–308. DOI: [10.3112/erdkunde.2009.04.01](https://doi.org/10.3112/erdkunde.2009.04.01)
- BENDIX, J.; ROLLENBECK, R.; RICHTER, M.; FABIAN, P. and EMCK, P. (2008): Climate. In: *Ecological Studies* 198, 63–73. DOI: [10.1007/978-3-540-73526-7_8](https://doi.org/10.1007/978-3-540-73526-7_8)
- BENDIX, J.; TRACHTE, K.; CERMAK, J.; ROLLENBECK, R. and NAUSS, T. (2009): Formation of convective clouds at the foothills of the tropical eastern Andes (South Ecuador). In: *Journal of Applied Meteorology and Climatology* 48, 1682–1695. DOI: [10.1175/2009JAMC2078.1](https://doi.org/10.1175/2009JAMC2078.1)

- BENDIX, J.; SILVA, B.; ROOS, K.; GÖTTLICHER, D.; ROLLENBECK, R.; NAUSS, T. and BECK, E. (2010): Model parameterization to simulate and compare the PAR absorption potential of two competing plant species. In: *International Journal of Biometeorology* 54, 283–295. DOI: [10.1007/s00484-009-0279-3](https://doi.org/10.1007/s00484-009-0279-3)
- BONAN, G. B. (2008): Forests and climate change: forcings, feedbacks, and the climate benefits of forests. In: *Science* 320, 1444–1449. DOI: [10.1126/science.1155121](https://doi.org/10.1126/science.1155121)
- BRUIJNZEEL, L. A., MULLIGAN, M. and SCATENA, F. N. (2011): Hydrometeorology of tropical montane cloud forests: emerging patterns. In: *Hydrological Processes* 25, 465–498. DOI: [10.1002/hyp.7974](https://doi.org/10.1002/hyp.7974)
- BUYTAERT, W.; WYSEURE, G.; DE BIEVRE, B. and DECKERS, J. (2005): The effect of land-use changes on the hydrological behaviour of Histic Andosols in south Ecuador. In: *Hydrological Processes* 19, 3985–3997. DOI: [10.1002/hyp.7974](https://doi.org/10.1002/hyp.7974)
- CARDINALE, B. J.; DUFFY, J. E.; GONZALEZ, A.; HOOPER, D. U.; PERRINGS, C.; VENAIL, P.; NARWAN, A.; MACE, G. M.; TILMAN, D.; WARDLE, D. A.; KINZIG, A. P.; DAILY, G. C.; LOREAU, M.; GRACE, J. B.; LARIGAUDERIE, A.; SRIVASTAVA, D. S. and NAEEM, S. (2012): Biodiversity loss and its impact on humanity. In: *Nature* 486, 59–67. DOI: [10.1038/nature11148](https://doi.org/10.1038/nature11148)
- CURATOLA FERNÁNDEZ, G. F.; SILVA, B.; GAWLIK, J.; THIES, B. and BENDIX, J. (2013): Bracken fern frond status classification in the Andes of southern Ecuador: combining multispectral satellite data and field spectroscopy. In: *International Journal of Remote Sensing* 34, 7020–7037. DOI: [10.1080/01431161.2013.813091](https://doi.org/10.1080/01431161.2013.813091)
- CURATOLA FERNÁNDEZ, G. F.; OBERMEIER, W. A.; GERIQUE, A.; LÓPEZ SANDOVAL, M. F.; LEHNERT, L. W.; THIES, B. and BENDIX, J. (2015): Land cover change in the Andes of southern Ecuador – patterns and drivers. In: *Remote Sensing* 7, 2509–2542. DOI: [10.3390/rs70302509](https://doi.org/10.3390/rs70302509)
- DA SILVA, J. M. and ARRABACA, M. C. (2004): Photosynthesis in the water-stressed C_4 grass *Setaria sphacelata* is mainly limited by stomata with both rapidly and slowly imposed water deficits. In: *Physiologia Plantarum* 121, 409–420. DOI: [10.1111/j.1399-3054.2004.00328.x](https://doi.org/10.1111/j.1399-3054.2004.00328.x)
- EITZOLD, S.; BUCHMANN, N. and EUGSTER, W. (2010): Contribution of advection to the carbon budget measured by eddy covariance at a steep mountain slope forest in Switzerland. In: *Biogeosciences* 7, 2461–2475. DOI: [10.5194/bg-7-2461-2010](https://doi.org/10.5194/bg-7-2461-2010)
- FARQUHAR, G. D.; EHLERINGER, J. R. and HUBICK, K. T. (1989): Carbon isotope discrimination and photosynthesis. In: *Annual Review of Plant Physiology and Plant Molecular Biology* 40, 503–537. DOI: [10.1146/annurev.pp.40.060189.002443](https://doi.org/10.1146/annurev.pp.40.060189.002443)
- FLEISCHBEIN, K.; WILCKE, W.; GOLLER, R.; VALAREZO, C.; ZECH, W. and KNOBLICH, K. (2011): Measured and modeled rainfall interception in a lower montane forest, Ecuador. In: BRUIJNZEEL, L. A.; SCATENA, F. N. and HAMILTON, L. S. (eds): *Tropical montane cloud forests: science for conservation and management*. Cambridge, 309–316. DOI: [10.1017/CBO9780511778384.034](https://doi.org/10.1017/CBO9780511778384.034)
- GÖTTLICHER, D.; OBREGÓN, A.; HOMEIER, J.; ROLLENBECK, R.; NAUSS, T. and BENDIX, J. (2009): Land cover classification in the Andes of southern Ecuador using Landsat ETM+ data as a basis for SVAT modelling. In: *International Journal of Remote Sensing* 30, 1867–1886. DOI: [10.1080/01431160802541531](https://doi.org/10.1080/01431160802541531)
- HAMMERLE, A.; HASLWANTER, A.; SCHMITT, M.; BAHN, M.; TAPPEINER, U.; CERNUSCA, A. and WOHLFAHRT, G. (2007): Eddy covariance measurements of carbon dioxide, latent and sensible energy fluxes above a meadow on a mountain slope. In: *Boundary-layer Meteorology* 122, 397–416. DOI: [10.1007/s10546-006-9109-x](https://doi.org/10.1007/s10546-006-9109-x)
- HSIEH, C. I.; KATUL, G. and CHI, T. W. (2000): An approximate analytical model for footprint estimation of scalar fluxes in thermally stratified atmospheric flows. In: *Advances in Water Resources* 23, 765–772. DOI: [10.1016/s0309-1708\(99\)00042-1](https://doi.org/10.1016/s0309-1708(99)00042-1)
- HU, Z.; YU, G.; ZHOU, Y.; SUN, X.; LI, Y.; SHI, P.; WANG, Y.; SONG X.; ZHENG, Z.; ZHANG, L. and LI, S. (2009): Partitioning of evapotranspiration and its controls in four grassland ecosystems: application of a two-source model. In: *Agricultural and Forest Meteorology* 149, 1410–1420. DOI: [10.1016/j.agrformet.2009.03.014](https://doi.org/10.1016/j.agrformet.2009.03.014)
- KADEREIT, J. W.; KÖRNER, C.; KOST, B. and SONNEWALD U. (2014): *Lehrbuch der Pflanzenwissenschaften* 37. Heidelberg.
- KNOKE, T.; BENDIX, J.; POHLE, P.; HAMER, U.; HILDEBRANDT, P.; ROOS, K.; GERIQUE, A.; LOPEZ SANDOVAL, M.; BREUER, L.; TISCHER, A.; SILVA, B.; BALTAZAR, C.; AGUIRRE, N.; CASTRO, L. M.; WINDHORST, D.; WEBER, M.; STIMM, B.; GÜNTHER, S.; PALOMEQUE, X.; MORA, J.; MOSANDI, R. and BECK, E. (2014): Afforestation or intense pasturing improve the ecological and economic value of abandoned tropical farmlands. In: *Nature Communications* 5. DOI: [10.1038/ncomms6612](https://doi.org/10.1038/ncomms6612)
- LOPEZ-URREA, R.; DE SANTA OLALLA, F. M.; FÁBEBIRO, C. and MORATALLA, A. (2006): An evaluation of two hourly reference evapotranspiration equations for semiarid conditions. In: *Agricultural Water Management* 86, 277–282. DOI: [10.1016/j.agwat.2006.05.017](https://doi.org/10.1016/j.agwat.2006.05.017)
- LU, X. and ZHUANG, Q. (2010): Evaluating evapotranspiration and water-use efficiency of terrestrial ecosystems in the conterminous United States using MODIS and AmeriFlux data. In: *Remote Sensing of Environment* 114, 1924–1939. DOI: [10.1016/j.rse.2010.04.001](https://doi.org/10.1016/j.rse.2010.04.001)
- LUDLOW, M. M.; FISCHER, M. J. and WILSON, J. R. (1985): Stomatal adjustment to water deficits in three tropical grasses and a tropical legume grown in controlled conditions and in the field. In: *Australian Journal of Plant Physiology* 12 (2), 131–149. DOI: [10.1071/pp9850131](https://doi.org/10.1071/pp9850131)
- LUO, Y.; ZHAO, X.; ZHOU, R.; HUANG, Y. and ZUO, X. (2009): Photosynthetic performance of *Setaria viridis* to soil drought and rewetting alternations. In: *Sciences in Cold and Arid Regions* 1, 404–411.

- MAKOWSKI GIANNONI, S.; ROLLENBECK, R.; FABIAN, P. and BENDIX, J. (2013): Complex topography influences atmospheric nitrate deposition in a neotropical mountain rainforest. In: *Atmospheric Environment* 79, 385–394. DOI: [10.1016/j.atmosenv.2013.06.023](https://doi.org/10.1016/j.atmosenv.2013.06.023)
- MARTINS, C. A.; MORAES, O. L. L.; ACEVEDO, O. C. and DEGRAZIA, G. A. (2009): Turbulence intensity parameters over a very complex terrain. In: *Boundary-Layer Meteorology* 133, 35–45. DOI: [10.1007/s10546-009-9413-3](https://doi.org/10.1007/s10546-009-9413-3)
- MCMAHON, T. A.; PEEL, M. C.; LOWE, L.; SRIKANTHAN, R. and McVICAR, T. R. (2013): Estimating actual, potential, reference crop and pan evaporation using standard meteorological data: a pragmatic synthesis. In: *Hydrology and Earth System Sciences* 17, 1331–1363. DOI: [10.1007/s10546-009-9413-3](https://doi.org/10.1007/s10546-009-9413-3)
- MORAES, O. L. L.; ACEVEDO, O. C.; DEGRAZIA, G. A.; AFONSSI, D.; DA SILVA, R. and ANABOR, V. (2005): Surface layer turbulence parameters over a complex terrain. In: *Atmospheric Environment* 39, 3103–3112. DOI: [10.1016/j.atmosenv.2005.01.046](https://doi.org/10.1016/j.atmosenv.2005.01.046)
- ODHIAMBO, G. O. (2011): Comparison of surface layer scintillometer and eddy covariance footprint and sensible heat flux estimates for different wind directions. In: *Proceedings of 2nd International Conference on Environmental Science and Technology (ICEST 2011) IPCBEE Vol. 6, V1-355–V1-360*. Singapore.
- ODHIAMBO, G. O. and SAVAGE, M. J. (2009): Surface layer scintillometry for estimating the sensible heat flux component of the surface energy balance. In: *South African Journal of Science* 105, 208–216.
- OKE, T. R. (2002): *Boundary layer climates*. London.
- PELÁEZ-SAMANIEGO, M. R.; GARCIA-PÉREZ, M.; CORTEZ, L. A. B.; OSCULLO, J. and OLMEDO, G. (2007): Energy sector in Ecuador: current status. In: *Energy Policy* 35, 4177–4189. DOI: [10.1016/j.enpol.2007.02.025](https://doi.org/10.1016/j.enpol.2007.02.025)
- ROLLENBECK, R. and BENDIX, J. (2011): Rainfall distribution in the Andes of southern Ecuador derived from blending weather radar data and meteorological field observations. In: *Atmospheric Research* 99, 277–289. DOI: [10.1016/j.atmosres.2010.10.018](https://doi.org/10.1016/j.atmosres.2010.10.018)
- SAVAGE, M. J. (2009): Estimation of evaporation using a dual-beam surface layer scintillometer and component energy balance measurements. In: *Agricultural and Forest Meteorology* 149, 501–517. DOI: [10.1016/j.agrformet.2008.09.012](https://doi.org/10.1016/j.agrformet.2008.09.012)
- SAVAGE, M. J.; ODHIAMBO, G. O.; MENGISTU, M. G.; EVERSON, C. S. and JARMAIN, C. (2010): Measurement of grassland evaporation using a surface-layer scintillometer. In: *Water SA* 36, 1–8. DOI: [10.4314/wsa.v36i1.50901](https://doi.org/10.4314/wsa.v36i1.50901)
- SILVA, B. and BENDIX, J. (2014): Remote sensing of vegetation in a tropical mountain ecosystem: individual tree-crown detection. In: *Proceedings of SPIE Vol. 8893, 88930B-1*. DOI: [10.1117/12.2029912](https://doi.org/10.1117/12.2029912)
- SILVA, B.; ROOS, K.; VOSS, I.; KÖNIG, N.; ROLLENBECK, R.; SCHEIBE, R.; BECK, E. and BENDIX, J. (2012): Simulating canopy photosynthesis for two competing species of an anthropogenic grassland community in the Andes of southern Ecuador. In: *Ecological Modelling* 239, 14–26. DOI: [10.1016/j.ecolmodel.2012.01.016](https://doi.org/10.1016/j.ecolmodel.2012.01.016)
- SILVA, B.; DISLICH, C.; VOSS, I.; ROOS, K.; SCHEIBE, R.; VORPAHL, P.; SCHRÖDER, B.; HUTH, A.; BECK, E. and BENDIX, J. (2013): Climate change and its impact on current and future vegetation dynamics and carbon cycling. In: *Ecological Studies* 221, 331–342. DOI: [10.1007/978-3-642-38137-9_24](https://doi.org/10.1007/978-3-642-38137-9_24)
- THIERMANN, V. and GRASSI, T. (1992): The measurement of turbulent surface-layer fluxes by use of bichromatic scintillation. In: *Boundary-Layer Meteorology* 58, 367–389. DOI: [10.1007/bf00120238](https://doi.org/10.1007/bf00120238)
- THIES, B.; MEYER, H.; NAUSS, T. and BENDIX, J. (2014): Projecting land use and land cover changes in a tropical mountain forest of Southern Ecuador. In: *Journal of Land Use Science* 9, 1–33. DOI: [10.1080/1747423X.2012.718378](https://doi.org/10.1080/1747423X.2012.718378)
- WINDHORST, D.; KRAFT, P.; TIMBE, E.; FREDE, H. and BREUER, L. (2014): Stable water isotope tracing through hydrological models for disentangling runoff generation processes at the hillslope scale. In: *Hydrology and Earth System Sciences* 18, 4113–4127. DOI: [10.5194/hess-18-4113-2014](https://doi.org/10.5194/hess-18-4113-2014)
- YEPEZ, E. A.; HUXMAN, T. E.; IGNACE, D. D.; ENGLISH, N. B.; WELTZIN, J. F.; CASTELLANOS, A. E. and WILLIAMS, D. G. (2005): Dynamics of transpiration and evaporation following a moisture pulse in semiarid grassland: a chamber-based isotope method for partitioning flux components. In: *Agricultural and Forest Meteorology* 132, 359–376. DOI: [10.1016/j.agrformet.2005.09.006](https://doi.org/10.1016/j.agrformet.2005.09.006)

Authors

Prof. Dr. Jörg Bendix
 Dr. Brenner Silva
 University of Marburg
 Faculty of Geography
 Deutschhausstr. 10
 35032 Marburg
bendix@staff.uni-marburg.de
silvab@staff.uni-marburg.de

Prof. Dr. Erwin Beck
 Dr. Simone Strobl
 University of Bayreuth
 Faculty for Biology, Chemistry and
 Geosciences
 Universitätsstr. 30
 95440 Bayreuth
erwin.beck@uni-bayreuth.de
simone.strobl@uni-bayreuth.de